2012

Nanodiscs via interfacial cross-linking of smectic liquid-crystalline phase and their application

Chia-Yu Shen
Iowa State University

Nanodiscs via interfacial cross-linking of smectic liquid-crystaline phase and their applications

by

Chia-Yu Shen

A thesis submitted to graduate faculty

in partial fulfillment of the requirements for the degree of

MASTER OF SCIENCE

Major: Organic Chemistry

Program of Study Committee

Yan Zhao, Major Professor

Nicola Pohl

Malika Jeffries-EL

Iowa State University

Ames, Iowa

2012

Table of Contents

Chapter 1. GENERAL INTRODUCTION

1.1 Thesis organization

The five chapters of this thesis describe a nanodisc material formed by the photocross-linking of a surfactant molecule. The nanodiscs were formed by the interfacial cross-linking of a newly synthesized surfactant in the hydrophilic region in the lyotropic liquid crystal phase.

Chapter 1 is a general introduction that reviews self-assembled structures formed by amphiphiles and how polymerization stabilizes bilayer vesicles and inverse hexagonal liquid crystalline phase in particular.

Chapter 2 is on the photocross-linking of a lyotropic liquid crystal formed by triallyl(3,4,5-tridodecyloxybenzyl)ammonium bromide. The liquid crystal was characterized by XRD (powder x-ray diffraction) and PLM (polarized light microscopy). The cross-linked material was characterized by TEM (transmission electron microscopy) and AFM (atomic force microscopy).

Chapter 3 focuses on the ability of the above cross-linked nanodiscs to transport hydrophilic molecules across nonpolar phases. U-tube experiments were used to explore the transport efficiency and selectivity of the transport.

Chapter 4 is about the potential applications of nanodiscs in catalysis. The nanodisc was able to extract anionic catalysts from an aqueous phase to its core. Various catalysts were examined with the idea of using the nanodiscs as a soluble support for the catalysts.

Chapter 5 draws some general conclusions and suggests some possible future work,

including the applications of the nanodiscs in catalysis and possible modification of the surfactant to apply the cross-linking strategy to yield organic nanotubes.

1.2 Self-assembly of amphiphiles

Amphiphiles (Figure 1) are molecules having a hydrophilic (water-loving) headgroup and at least one hydrophobic (oil-loving) tail. Two of the simplest structures formed by surfactant are micelles and reverse micelles (Figure 2). In a micellar structure,[1] the amphiphiles keep their hydrophilic headgroups outward to be solvated by water and their hydrophobic tails in the core. In a reverse micelle,[2] the arrangement of the amphiphiles is just the opposite, with the hydrophilic headgroups pointing inward around a water pool and the hydrophobic tails outward to interact with the organic solvent. Both micellar and reverse micellar structures are useful as templates for the synthesis of inorganic nanomaterials.[3] Their applications in drug delivery[4] and catalysis[5] have also been reported.

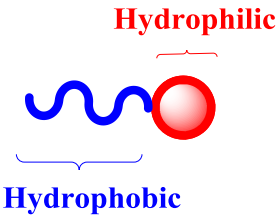

Figure 1. Schematic representation of an amphiphile, showing a hydrophilic headgroup and a hydrophobic tail.

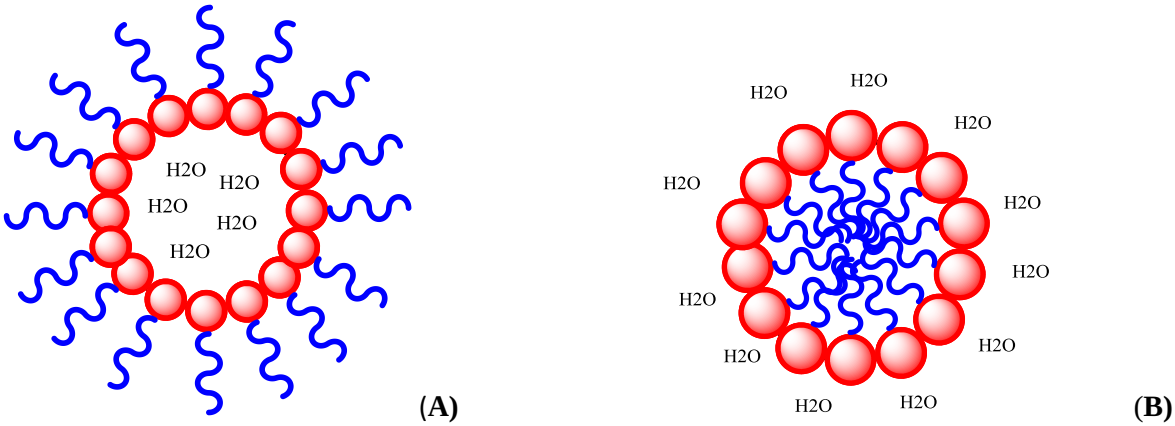

Figure 2. The structure of (A) a micelle and (B) a reverse micelle.

Lyotropic liquid crystals (LLC) are structures formed when amphiphilic molecules and solvents are mixed.[6] Hydrated amphiphiles can form various liquid-crystalline phases, depending on the structure of amphiphile, temperature, the amount of water, and the concentration of the amphiphiles.[7] Reported phases include lamellar, bicontinuous cubic, and hexagonal/cylindrical phases. Although LLC phases (Figure 3) are ordered nanostructures, their noncovalent nature in structures make them easily disturbed by chemical and physical forces.[7,8] For this reason, stabilizing the LLC structures via polymerization has been studied intensively in the past decade.[7,9]

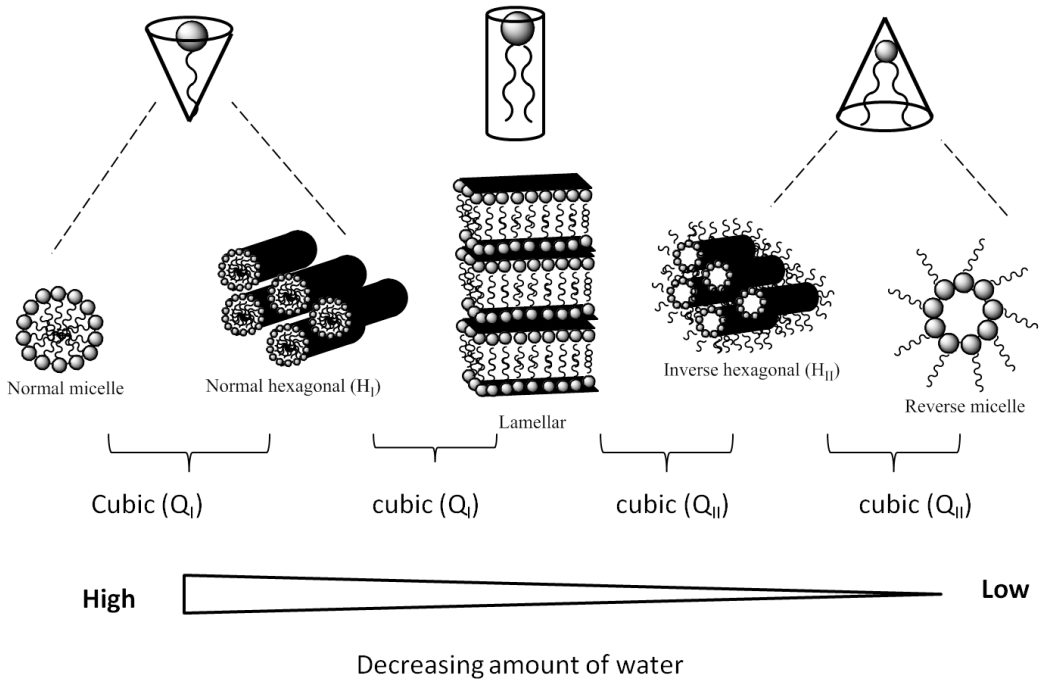

Figure 3. Structures of micellar, reverse micellar, lamellar, cubic, and hexagonal structures formed by amphiphile, dependent upon the water content and shape of the amphiphile.

1.3 Polymerization of lamellar structure

Polymerizable amphiphiles have been synthesized for covalent capture of LLCs.[7] Functional groups that have been applied in the polymerization of lamellar LLCs include diacetylenyl, dienoyl, sorbyl, acryloyl, and methacryloyl groups (Chart 1). Generally, these functional groups successfully stabilized fluid lamellar LLCs (L_α) via cross-linking in hydrophobic regions because L_α has rapid lateral diffusion which facilitates the polymerization process.[7]

The O'Brien's group has studied a series of similar amphiphiles incorporating acryloyl,[10] methacryloyl,[11] or sorbyl group[12] into hydrophobic tail of lipid molecule. Phospholipids are characterized by a polar headgroup and two hydrocarbon tails. The most common self-assembled structure formed by phospholipids is a vesicle, which consists of a water pool surrounded by a bilayer membrane. With polymerizable groups on the hydrophobic tail, polymerization can be easily confined within the lipid bilayers and help stabilize the vesicles.

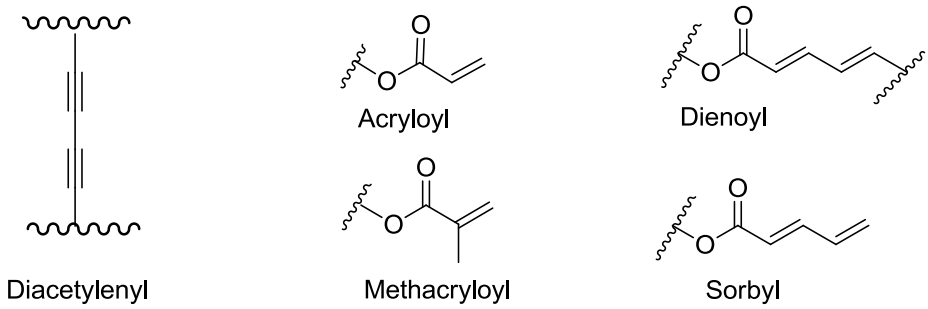

Chart 1. Various polymerizing groups studied to polymerize lamellar LLC structure.

Although the polymerization of lipid-bilayer vesicles is well-confined in hydrophobic region, the efficiency of polymerization and the integrity of structure are still influenced by different polymerizable groups. A brief review of the functional groups in chart 1 can help the selection of the group to polymerize non-lamellar structures. For example, although it is easy to detect the polymerization process by observing color change of the diacetylenyl group, the diacetylenyl group can only be applied to limited structures. After polymerization, the diacetylenyl group forms topotactic backbone consisting of conjugated alternating double and triple bonds, and this topotactic nature of poly-(diacetylene) tends to disturb the original

liquid crystalline structures,[13] which is not suitable for some structure sensitive liquid crystals. Both acryloyl and methacryloyl groups can be usefully employed in the rapid-diffusing liquid-like and slow-diffusing solid-like bilayer phase, as they are efficient in radical chain polymerization.[14] Dienoyl and sorbyl groups have similar properties to those of the acyloyl and methacryloyl groups, although a moderate degree of order in a structure is needed to incorporate dienoyl and sorbyl groups for polymerization.[15] Their easy cross-linking makes them readily used in photopolymerization, thermal initiation, and redox initiation.

1.4 Polymerization of inverse hexagonal phase (H_{II} phase)

Covalent capture of nonlamellar structures such as inverse hexagonal phase (H_{II}[16]) (Figure 3) has also been studied, although not as many successful examples have been reported as the capture of the lamellar phase. Some of the functional groups applied in polymerizing lamellar phase successfully cross-linked H_{II} phase in the hydrophobic region, including acryloyl,[16] diene[17] and styryl[18] groups. A good example of polymerizing H_{II} phase is reported by the Gin group.[16] The Gin's amphiphile (**1**) is cone-shaped with a small hydrophilic headgroup and a wedge-like, hydrophobic moiety. Three acryloyl groups are located at the ends of the hydrophobic tails and enable cross-linking while the amphiphiles pack into columns in the reverse micellar form. As a result, the polymerized H_{II} phase is a polymeric film with hydrophilic channels in the interior. Such films have been used for nanofiltration[19], catalyst support,[20] and template synthesis[21] of inorganic material by the Gin's group.

Polymerizing H_{II} phase via hydrophobic cross-linking can help maintain nano-columnar structures, but the nanocolumns are connected covalently and cannot form individual organic nanotubes in organic solvent. Accordingly, polymerization of H_{II} phase via hydrophobic region limits the use of self-assembled columns in organic nanotubes formation. To solve this problem, polymerization via hydrophilic region or near water pool region is possible to synthesize individual cross-linked nanotubes by polymerizing the H_{II} phase. However, internal cross-linking of organic nanotubes in the H_{II} phase was rarely studied and there is no successful example.

The O'Brien group has attempted to cross-link organic nanotubes in the H_{II} phase.[22] A phosphoethanolamine lipid (**2**) was the amphiphile to form inverse hexagonal phase under the proper amount of lipid, water, and temperature. Dienoyl group was used as a polymerizable group and located on hydrophobic region but next to the hydrophilic headgroup of lipid, so the polymerization via dienoyl group was anticipated to fix the H_{II} phase and possibly form individual organic tubes. However, the result was not successful. Dienoyl groups next to hydrophilic headgroups polymerized H_{II} phase into a polymer film instead of individual columns because the polymer film is difficult to dissolve in most of organic solvents. According to O'Brien's result, the location of a polymerizable group next to a hydrophilic headgroup in hydrophobic region will still cross-link organic columns together instead of giving individually cross-linked organic columns.

Therefore, placing a polymerizable on the hydrophilic headgroup is possible to form internally cross-linked organic nanotubes in H_{II} phase via polyermization in hydrophilic region. However, this polymerizable group should be hydrophilic, not disturbing the polarity

of an amphiphile. Recently, the Zhao group has developed a surfactant for internal cross-linking of reverse micelles[23] by applying the thiol-ene click chemistry.[24] In their design (**3** and **4**), a quartanary ammonium headgroup with three allyl functional groups is the hydrophilic polymerizable group. The triallyl ammonium surfactant showed high cross-linking efficiency in reverse micelle structure with DTT (dithiotheitol) as a crosslinker, and the cross-linked reverse micelle can survive solvent changes and removal of solvents. Accordingly, a suitable surfactant bearing the triallyl ammonium headgroup might form internally cross-linked nanotubes via polymerization in the H_{II} phase. In this thesis, a new surfactant with a triallyl ammonium headgroup was studied to see whether it could form individual cross-linked nanotubes in the H_{II} liquid-crystalline phase.

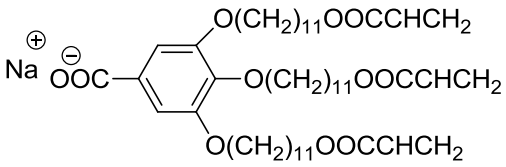

1

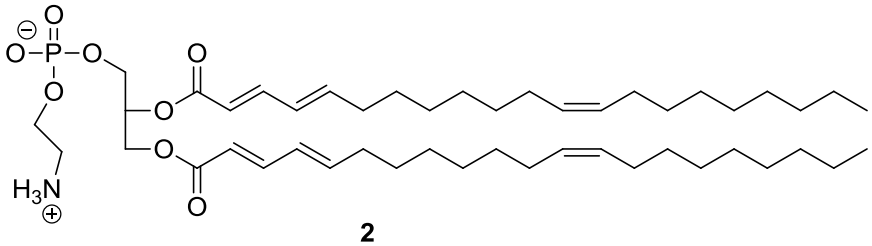

2

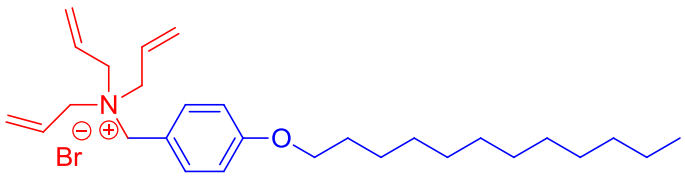

3

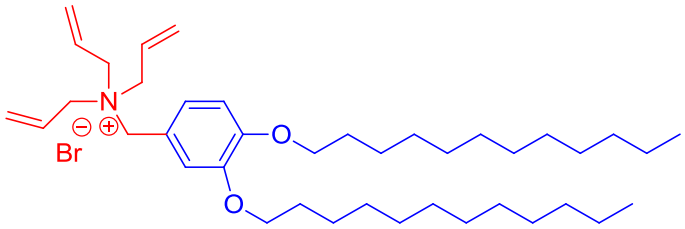

4

1.5 References

(1) Khanal, A.; Inoue, Y.; Yada, M.; Nakashima, K. *J. Am. Chem. Soc*. **2007**, *129*, 1534.

(2) Qi, L.; Ma, J.; Cheng, H.; Zhao, Z. *J. Phys. Chem. B*. **1997**, *101*, 3460.

(3) (a) Qi, L.; Ma, J.; Cheng, H.; Zhao, Z. *J. Phys. Chem. B*. **1997**, *101*, 3460. (b) Sugimoto, T.; Kimijima, K.; *J. Phys. Chem. B*. **2003**, *107*, 10753. (c) Khanal, A.; Inoue, Y.; Yada, M.; Nakashima, K. *J. Am. Chem. Soc*. **2007**, *129*, 1534.

(4) Emoto, K.; Iijima, M.; Nagasaki, Y.; Kataoka, K. *J. Am. Chem. Soc.* **2000**, *122*, 2653-2654.

(5) (a) Buriak, J. M.; Osborn, J. A. *Organometallics*. **1996**, *15*, 3161. (b) Meric, P.; K. Yu, K.M.; Tsang, S. C. *Langmuir*. **2004**, *20*, 8537. (c) Wang, F.; Lin, H.; Cun, L.; Zhu, J.; Deng, J.; Jiang, Y. *J. Org. Chem*. **2005**, *70*, 9424.

(6) Figueiredo Neto, A.M.; Salinas, S.A. *The Physics of Lyotropic Liquid Crystals: Phase Transitions and Structural Properties*. Oxford Science Press. New York. 2005.

(7) Mueller, A.; O'Brien, D.F. *Chem.Rev*. **2002**, *102*, 727.

(8) (a) Gin, D.L.; Gu, W.; Pindzola, B.A.; Zhou, W.J. *Acc.Chem.Res.* **2001**, *34*, 973. (b) Gray, D.H.; Hu, S.; Juang, E.; Gin, D.L. *Adv. Mater. Mater*. **1997**. *9*. 731.

(9) O'Brien, D.f.; Armitage, B.; Benedicto, A.; Bennett, D.E.; Lamparski, H.G.; Lee, Y.-S.; Srisiri, W.; Sission, T.M. *Acc. Chem. Res*. **1998**, *31*, 861.

(10) Sells, T. D.; O'Brien, D. F. *Macromolecules*, **1994**, *27*, 226-233.

(11) Lei, J.; O'Brien, D. F. *Macromolecules*, **1994**, *27*, 1381-1388.

(12) Lamparski, H.; O'Brien, D. F. *Macromolecules*, **1995**, *28*, 1786-1794.

(13) Day, D.; Ringsdorf, H. *J. Polym. Sci*. **1978**. *16*. 205.

(14) Lei, J.; Sisson, T. M.; Lamparski, H. G.; O'Brien, D. F. *Macromolecules*, **1999**, *32*, 73-78.

(15) (a) Barraud, A.; Rosilio, C.; Ruaudel-Teixier, A. *Thin Solid Films.* **1980**, *68*, 7-12. (b) Ringsdorf, H.; Schupp, H. *J. Macromol. Sci. Chem.* **1988**, *21*, 1936-1941.

(16) Smith,R. C.; Fischer, W.M.; Gin, D.L. *J. Am. Chem.Soc*. **1997**, *119*, 4092.

(17) Hoag, B. P.; Gin, D. L. *Macromolecules*, **2000**, *33*, 8549-8558.

(18) Gray, D. H.; Hu, S.; Juang, E.; Gin, D.L. *Adv. Mater*. **1997**, *9*, 731-736.

(19) Gin, D.L.; Lu, X.; Nemade, P.R.; Pecinovsky, C.S.; Xu, Y.; Zhou, M. *Adv. Func. Mater*. **2006**, *16*, 865.

(20) (a) Miller, S.A.; Kim, E.; Gray, D.H.; Gin, D.L. *Angew. Chem. Int. Ed*. **1999**, *38*, 3021. (b) Ding, J.H.; Gin, D.L. *Chem. Mater*. **2000**, *12*, 22.

(21) Gray, D.H.; Gin, D.L. *Chem. Mater*. **1998**, *10*, 1827.

(22) Srisiri, W.; Sisson, T. M.; O'Brien, D.F.; McGrath, K.M.; Han, Y.; Gruner, S.M. *J.Am. Chem. Soc*. **1997**, *119*, 4866.

(23) Zhang, S.; Zhao, Y. *ACS Nano*. **2011**, *5*, 2637.

(24) (a) Dondoni, A. *Angew. Chem. Int. Ed.* **2008**, *47*, 8995. (b) Hoyle. C. E.; Lee, T.Y.; Roper, T. *J. Polym. Sci. Part A: Polym. Chem*. **2004**, *42*, 5301. (c) Iha, R.K.; Wooley, K.L.; Nystrom, A. M.; Burke, D.J.; Kade, M.J.; Hawker, C.J. *Chem. Rev*. **2009**, *109*, 5620.

Chapter 2.NANODISCS FORMED BY PHOTOCROSS-LINKING OF TRIALLYL(3,4,5-TRIDODECYLOXYBENZYL)AMMONIUM BROMIDE

2.1 Abstract

In this chapter, triallyl(3,4,5- tridodecyloxybenzyl)ammonium bromide was used to form lyotropic liquid crystal. Inverted hexagonal phase was the original target. The liquid crystal and the cross-linked material were characterized by XRD (powder x-ray diffraction), PLM (polarized light microscopy), TEM (transmission electron microscopy), and AFM (atomic force microscopy). The characterizations indicated that the surfactant did not form inverse hexagonal phase but smectic phase instead. The cross-linking afforded nanodisc-like structures as a result.

The large size of the triallyl ammonium headgroup was possibly responsible for the phase change.

2.2 Introduction

Recently, the Zhao group has synthesized interfacially cross-linkable amphiphiles (**1** and **2**) with a triallyl ammonium headgroup.[1] These amphiphiles can form reverse micelles in nonpolar solvents containing a small amount of water. DTT (dithiothreitol) was used as a water-soluble cross-linker. Its hydrophilicity allowed it to be partially dissolved in the water pool of the reverse micelle. Because the high local concentrations of the allyl and thiol group near the amphiphile/water interface, the radical thiol-ene reaction[2] proceeded extremely rapidly, capturing the reverse micellar structures as a result. The resulting interfacially cross-linked reverse micelles (ICRMs) are core/shell nanoparticles and can be dissolved in common organic solvents such as chloroform. There are a few advantages for applying the

thiol-ene reaction in the cross-linking of reverse micelles.[1] First, the reaction is extremely efficient, giving high yields even in sterically congested systems such as dendrimers and selective functionalization of proteins. Second, it is simple to incorporate vinyl groups into amphiphiles. For example, three vinyl groups were easily incorporated into **1** and **2**. High density of cross-linkable groups can enhance the cross-linking efficiency at the core and is advantageous to the stability of the cross-linked micelle. Third, great flexibility exists in the structure of thiol-ene cross-linkers. If cross-linkers with appropriate lengths are used, the cross-linking should cause minimal perturbation to the packing of the surfactants. In contrast, free-radical polymerization of vinyl monomers tends to make the structure more compact.

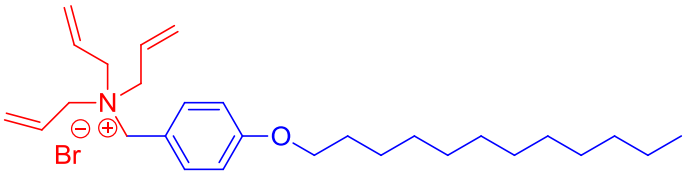

1

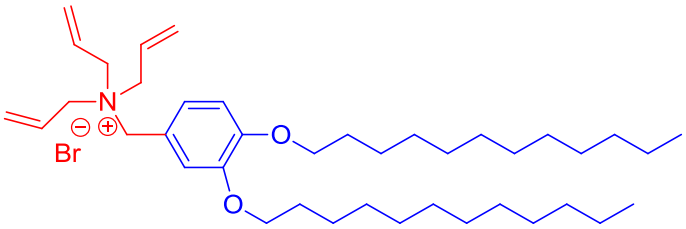

2

We thought the same strategy could be used to capture other liquid crystalline phases. In particular, we are interested in the cross-linking of the reverse hexagonal phase because cross-linking near the polar headgroups should afford organic nanotubes in a straightforward fashion.

The design of surfactant for H_{II} phase is mainly based on the packing parameter which is related to the molecular geometry. According to Israelachvili,[3] the packing parameter is defined as $Q = v/a_0 l_c$, in which v is the volume of hydrophobe of a surfactant, l_c the critical chain length, and a_0 the optimal head group area. With $Q < 1/3$, surfactants would form micellar structures because the size of the headgoup is much larger than that of the tail. With $1/2 < Q < 1$, bilayered vesicles are favored. With $Q \sim 1$, the shape of surfactant is a cylinder and planar bilayer is normally favored. With $Q > 1$, the hydrophobe is much larger than headgroup, inverted micellar structures are favored (Figure 3 in chapter 1). To obtain inverse hexagonal liquid crystal phase, one typically needs to employ wedge-like molecules such as **3** and **4**.[4,5] The large hydrophobe created by the three hydrocarbon tails makes the molecule pack into parallel columns in the hexagonal phase.

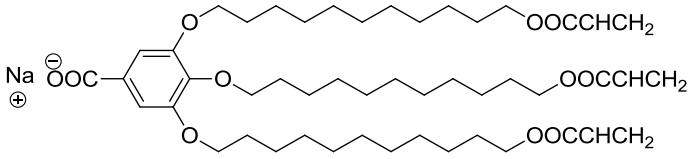

3

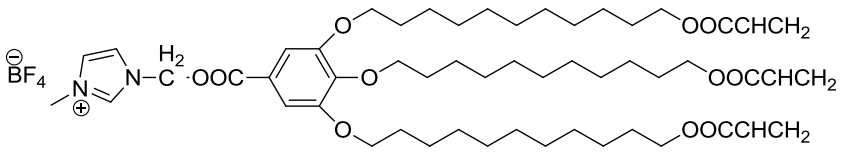

4

Because the amount of water to form H_{II} phase is very little, it is difficult to dissolve the required amount of water-soluble cross-linker DTT. Instead, we used organic soluble cross-linker, 1,3- propanedithiol. The expectation was that 1,3-propanedithiol would diffuse

into the interior of the columns formed by the self-assembled **5**, allowing the thiol-ene click chemistry to take place in the hydrophilic region.

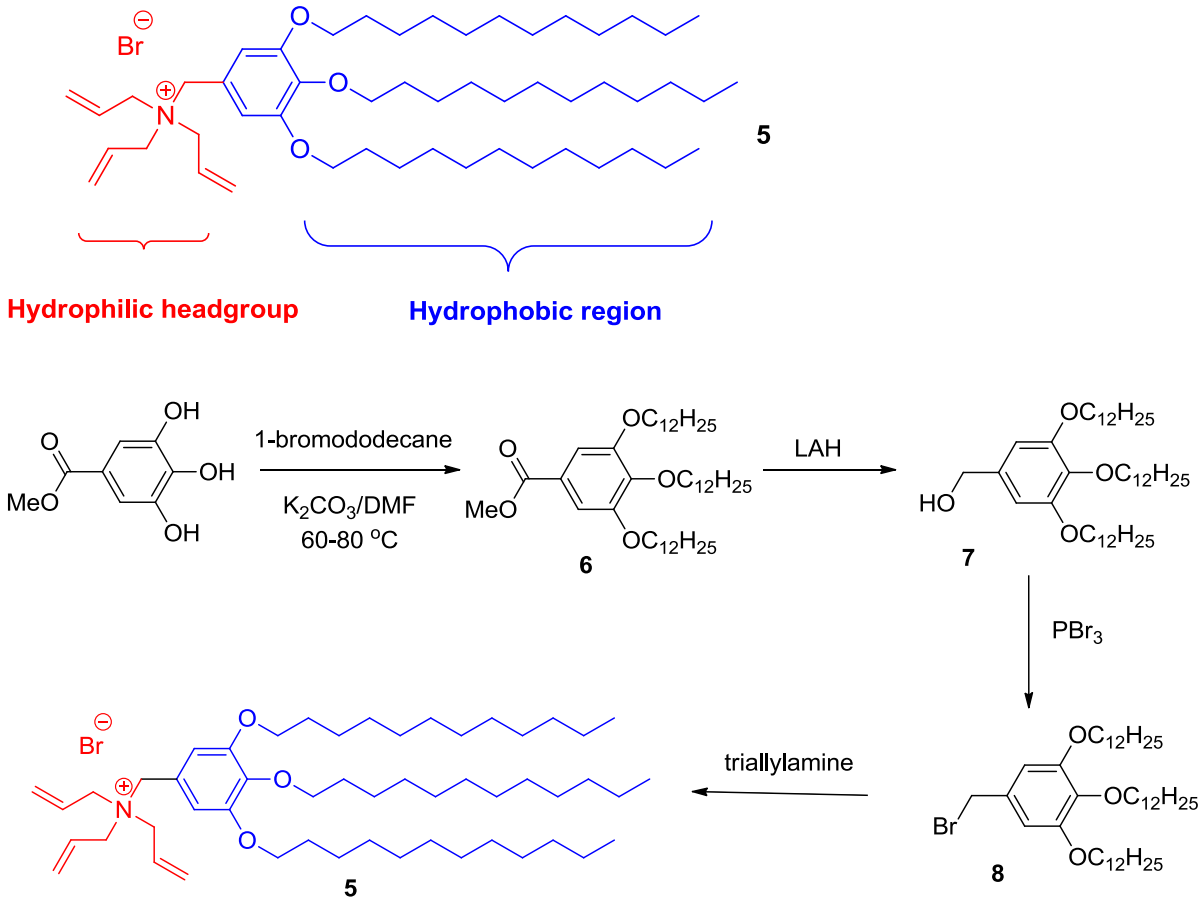

Scheme 1. Synthetic route of surfactant **5**.

2.3 Experimental section

General.

Common reagents and starting materials are purchased from Sigma-Aldrich Co. and Fisher Scientific Co. and used without further purification. The ^{1}H and ^{13}C NMR spectra were recorded at ambient temperature on a Varian MR400 instrument, with $CDCl_3$ as the

solvent and the solvent peak at 7.26 ppm used as the reference. DLS studies were performed on a PDDLS/Cool Batch 90 T dynamic light scattering detector at 25 ^{o}C. The intensity data were analyzed with the PRECISION DECONVOLVE program, and the size measurement was based on five replicates. UV data were recorded at ambient temperature on a Varian Cary Bio 50 UV-visible spectrophotometer. Transmission electron microscopy (TEM) studies were carried out on a PHILIPS CM30 instrument, operating at 150 kV.

Methyl-3,4,5-tris(dodecyloxy)benzoate (6). Potassium carbonate (23.8 g, 172.20 mmol) was added to a solution of methyl 3,4,5-trihydroxybenzoate (5.1 g, 27.54 mmol) in DMF (150 mL) at room temperature. After the mixture was stirred at 60 ^{o}C for 2 h, 1-bromododecane (21.30 mL, 88.03 mmol) was added slowly. Then the reaction mixture was stirred overnight at 80 ^{o}C, cooled to room temperature, and poured over 750 mL of icy water. The mixture was collected by vacuum filtration and recrystallized from 100 mL of acetone to give a yellow solid (20.0 g, 100%). ^{1}H NMR (400 MHz, $CDCl_3$, δ): 7.24 (s, 2 H), 3.99 (t, 6 H), 3.88 (s, 3 H), 1.82-1.25 (m, 60 H), 0.86 (t, 9 H).

3, 4, 5-Trisdodecyloxybenzyl alcohol (7). A solution of methyl-3,4,5-tris(dodecyloxy)-benzoate **8** (16.3 g, 23.60 mmol) in THF (125 mL) was added dropwise to a stirred suspension of (1.5 g, 38.74 mmol) in dry THF (40 mL) at 0 ^{o}C. The reaction was stirred overnight at room temperature and was quenched by methanol (10 mL) and water (10 mL). The solid formed was removed by filtration and the filtrate was concentrated *in vacuo*. The residue was dissolved in $CHCl_3$ (250 mL). The resulting solution was washed with water (2 ×100 mL), brine (2 × 100 mL), dried over anhydrous $MgSO_{4(s)}$, and concentrated *in vacuo*

to give a white solid (11.0 g, 71%). ^{1}H NMR (400 MHz, $CDCl_3$, δ): 6.56 (s, 2H), 4.59 (s, 2H),4.02-3.88 (m, 6H), 1.86-1.26 (m, 60H), 0.88 (t, 9H).

3, 4, 5-Trisdodecyloxybenzyl bromide (8). A solution of PBr_3 (0.5 mL, 5.32 mmol) in $CHCl_3$ (10 mL) was slowly added to a stirred solution of 3, 4, 5-tris(dodecyloxy)benzyl alcohol **7** (1.8 g, 2.67 mmol) in $CHCl_3$ (90 mL) at 0 ^{o}C. The reaction mixture was stirred at room temperature, monitored by TLC, and poured into water (250 mL). The product was extracted with $CHCl_3$ (2 × 50 mL). The combined organic phase was washed with brine (2 × 20 mL), dried over anhydrous $MgSO_4$(s), and concentrated *in vacuo* to give a white solid (1.7 g, 89%). ^{1}H NMR (400 MHz, $CDCl_3$, δ): 6.57 (s, 2H), 4.43 (s, 2H), 3.98-3.94 (m, 6H), 1.8-1.26 (m, 60H), 0.88 (t, 9H).

Triallyl(3,4,5-trisdodecyloxybenzyl)ammonium bromide (5). Triallylamine (1.8 mL, 10.36 mmol) was slowly added to a solution of 3, 4, 5-tris(dodecyloxy)benzyl bromide **6** (7.4 g, 10.27 mmol) in $CHCl_3$. After 3 d at room temperature, $CHCl_3$ was removed *in vacuo* and the crude product was washed with acetone (2 mL) to give a white solid (6.4 g, 72 %). ^{1}H NMR (400 MHz, $CDCl_3$, δ): 6.9 (s, 2H), 5.99-5.94 (m, 3H), 5.76-5.67 (m, 6H), 4.89 (s, 2H), 4.19(d, 6H).99-3.97 (m, 6H), 1.8-126 (m, 60H), 0.88 (t, 9H). ^{13}C NMR (400 MHz, $CDCl_3$, δ): 153.51, 140.00, 128.38, 125.30, 122.04, 111.53, 73.50, 69.61, 64.42, 61.89, 54.43, 31.95, 30.39, 29.79, 29.77, 29.75, 29.70, 29.68, 29.64, 29.62, 29.53, 29.44, 29.43, 29.42, 29.40, 26.20, 26.13, 22.71, 14.14. HR-MS (*m/z*) $[M\text{-}Br]^+$ for calcd $C_{52}H_{94}NO_3^+$, 780.7; found, 780.7.

Preparation of crosslinked nanomaterial through LC formation[4]

Triallyl(3,4,5-tridodecyloxybenzyl)ammonium bromide **5** (504.0 mg, 0.59 mmol), *p*-xylene (72.2 μL), nanopure water (42.1 μL), 2,2'-dimethoxy-2-phenylacetophenone (20 mol %, dissolved in *p* -xylene), and 1,3-propanedithiol (88.1 μL) were combined in a 50-mL glass centrifuge tube. The mixture was centrifuged at 2800 rpm for 10 min, followed by hand-mixing with a spetula at 50 ^{o}C. The procedure was repeated three times until a homogeneous mixture was formed. The temperature of the mixture was maintained at 50 ^{o}C for 1 h and the mixture was irradiated in Rayonet photoreactor overnight to ensure complete polymerization. The extent of the polymerization was confirmed by ^{1}H NMR spectroscopy. The phase architecture was confirmed by X-ray diffraction and polarized light microscopy.

Experimental procedure of XRD characterization

X-ray diffraction patterns were obtained using a Rigaku Ultima IV powder X-ray diffractometer with Bragg-Brentano geometry and a graphite crystal monochrometer. The power output of the Cu Kα target (λ = 1.5419 Å) was maintained at 1.76 kW. The viscous samples were spread on the back of a standard glass sample holder and analyzed.

Experimental procedure of AFM characterization

A Dimension 3100 from Digital Instruments/Veeco/Bruker (Santa Barbara, CA) equipped with a G scanner was utilized for topography image collection. The samples were imaged in Tapping mode using TESPA probes (Bruker, Santa Barbara, CA) under ambient conditions. Images were flattened before analysis.

Experimental procedure of PLM characterization

Images were captured with a Zeiss Axiocam MRc digital camera mounted on a Zeiss Axioplan II compound research microscope in the polarized light imaging mode (specimen viewed between crossed polarizers).

2.4 Results and discussion

XRD is a common characterization for liquid crystalline structures. Different liquid crystalline structures show different diffraction patterns, and it is possible to assign a liquid crystalline structure from a clear x-ray diffraction pattern alone.[7] The liquid crystal made from triallyl(3,4,5- tridodecyloxybenzyl)ammonium bromide (compound **5**) showed a strong signal at 2 θ = 2.36^{o} and the corresponding *d* spacing was 3.70 nm. A weak signal was also observed at 2 θ = 4.68^{o} and the corresponding d spacing was 1.86 nm (Figure 1).

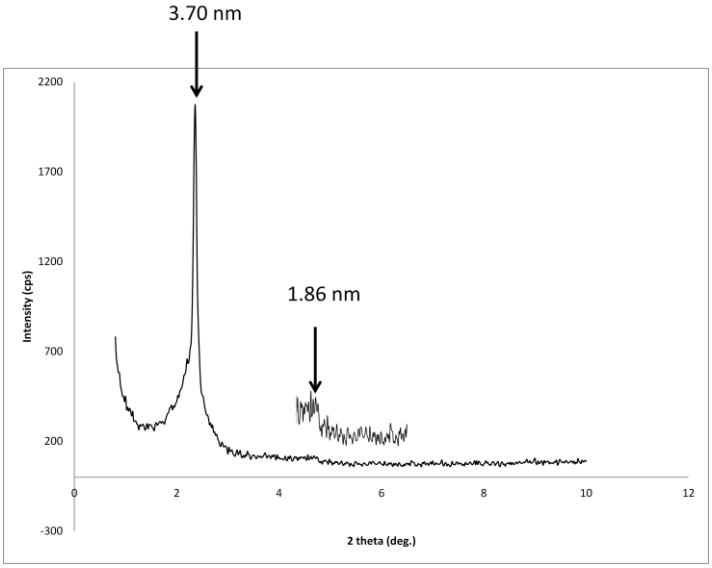

Figure 1. XRD of liquid crystal by surfactant **4**.

The liquid crystal was not H_{II} phase because the diffraction pattern does not match that of the H_{II} phase (the d-spacing ratio is 1, $1/\sqrt{3}$, $1/\sqrt{4}$ …, corresponding to d_{100}, d_{110}, d_{200}…). [7] Similarly, the cubic phase was ruled out.[8] It should be mentioned that, although compound **5** did not form the inverse hexagonal phase, it was not an isotropic mixture, which does not give any signals in x-ray diffraction. Other liquid crystalline structure must be formed by compound **5** instead of H_{II} phase.

Next, the lamellar phase was considered as the possible candidate, as it is next to H_{II} phase on the progression of the amount of water or the geometry of the amphiphiles (Figure 2). Although the diffraction pattern obtained was similar that of lamellar phase (1: 1/2: 1/3, …corresponding to d_{100}, d_{200}, d_{300}, …),[9] it is more ordered and generally has sharp signals at both the smaller and larger angles. In comparison, the liquid crystal of **5** shows a strong and sharp signal at the lower angle and a very weak signal at the higher angle, meaning it has order only in long distance, not in short distance.

Next, the x-ray diffraction patterns of the nematic[10] and smectic [7,11] phases were compared, because they are related to the lamellar phase. The smectic phase is composed of disc-like or cylindrical micelles or reverse micelles. Because these discs or cylinders aggregate in a layered fashion, there is resemblance between the smectic phase and the lamellar phase in x-ray diffraction pattern.[7,11] The x-ray diffraction pattern of the smectic phase is 1: 1/2 in d-spacing ratio, which is similar to the diffraction pattern of liquid crystal **5**. The strengths of the signals (i.e., strong at the lower angle and weak at the higher amgle) for the smectic phase indicated that this phase has more order in the long range than in the short range. Nematic phase[10] is also composed of discs and cylinders, but they aggregate in a

much less ordered fashion than smectic phase does. The corresponding diffraction pattern does not have sharp signals at lower and higher angles because nematic phase is not very organized. Overall, the XRD of amphiphile **5** suggests that the amphiphile most likely assembles into the smectic phase, although we cannot rule out the lamellar phase completely. The weakness of the high-angle signal, for example, may be affected by the quality of the liquid crystal.

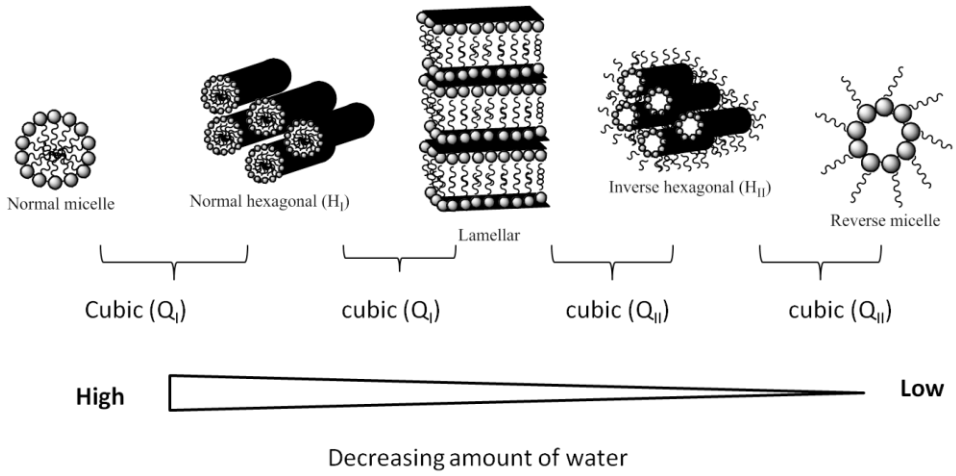

Figure 2. Some common liquid crystalline structures dependding on the amount of water.

PLM is another common method to characterize the structures of liquid crystals.[7] Different structures diffract polarized light in different ways, so the diffraction textures under the microscope are different and liquid crystalline structure can be characterized according to the specific diffraction textures.

The micrograph of the liquid crystal of **5** has a flower pattern with a fan-like texture with sharp fan tip (Figure 3). Nematic phase is excluded from candidate liquid crystalline structure because the PLM of nematic phase is thread-like structure,[9] which is totally

different from the PLM texture of liquid crystal of **5**. The PLM texture of lamellar liquid crystal is similar to the PLM texture of liquid crystal **5**.[12] Lamellar phase has so-called maltese crosses texture, which is flower pattern composed of four fans. One different characteristic from liquid crystal **5** is that the fan-like texture has round and smooth fan tips, not sharp ones. Compared to smectic phase, it was found that among different ordered smectic phases, smectic A (SmA) has the most similar texture in PLM characterization.[13] SmA has same flower pattern, and the fan-like texture has a sharp tip at the end of each fan. Accordingly, the smectic A phase is the most likely structure. Because the PLM images of **5** only differed in subtle ways from those of the lamellar phase, we still consider the latter a possibility.

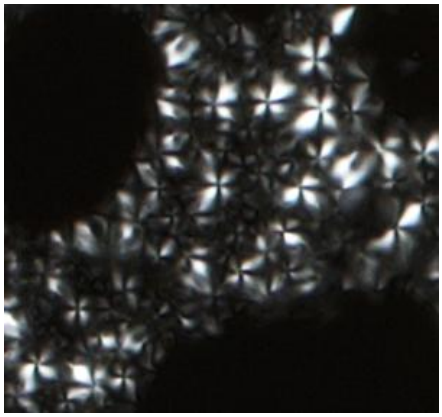

Figure 3. Polarized light microscopy of cross-linked liquid crystal by surfactant 4.

Photocross-linking

To monitor the progress of cross-linking in liquid crystal, ^{1}H NMR spectroscopy was used to examine the degree of cross-linking. One molar percent of photoinitiator (2,2'-dimethoxy-2-phenylacetophenone) relative to surfactant was used at first, and the result of cross-linking was poor as shown by the ^{1}H NMR spectroscopy. A possible reason for the low degree of cross-linking could be that the highly viscous liquid crystal makes the photoinitiator diffuse slowly, affecting the polymerization. To enhance the degree of cross-linking, more photoinitiators were added at 5, 10, 15, and 20 mol %, respectively. The higher photoinitiator loading did the cross-linking, as shown by the disappearance of the alkenic protons in the ^{1}H NMR spectra (Figure 4).

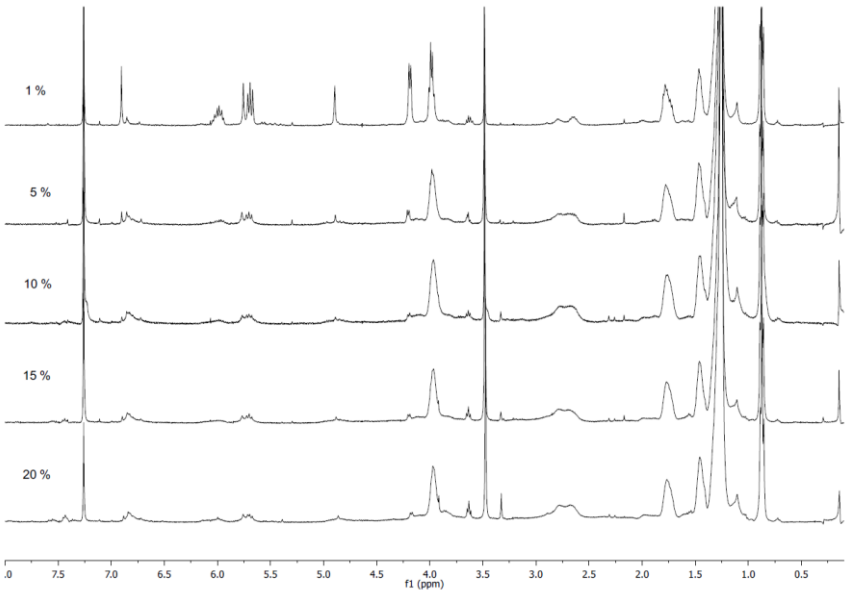

Figure 4. ^{1}H NMR progression according to increasing amount of photoinitiator.

The stability of the cross-linked materials with different amounts of photoinitiators was evaluated by DLS (dynamic light scattering). Only the cross-linked material with 20 mol %

of photoinitiator showed similar distribution of particle sizes before and after methanol washing. The size distribution of the materials is expected to change after methanol washing if the surfactants are not completely cross-linked (Figure 5).

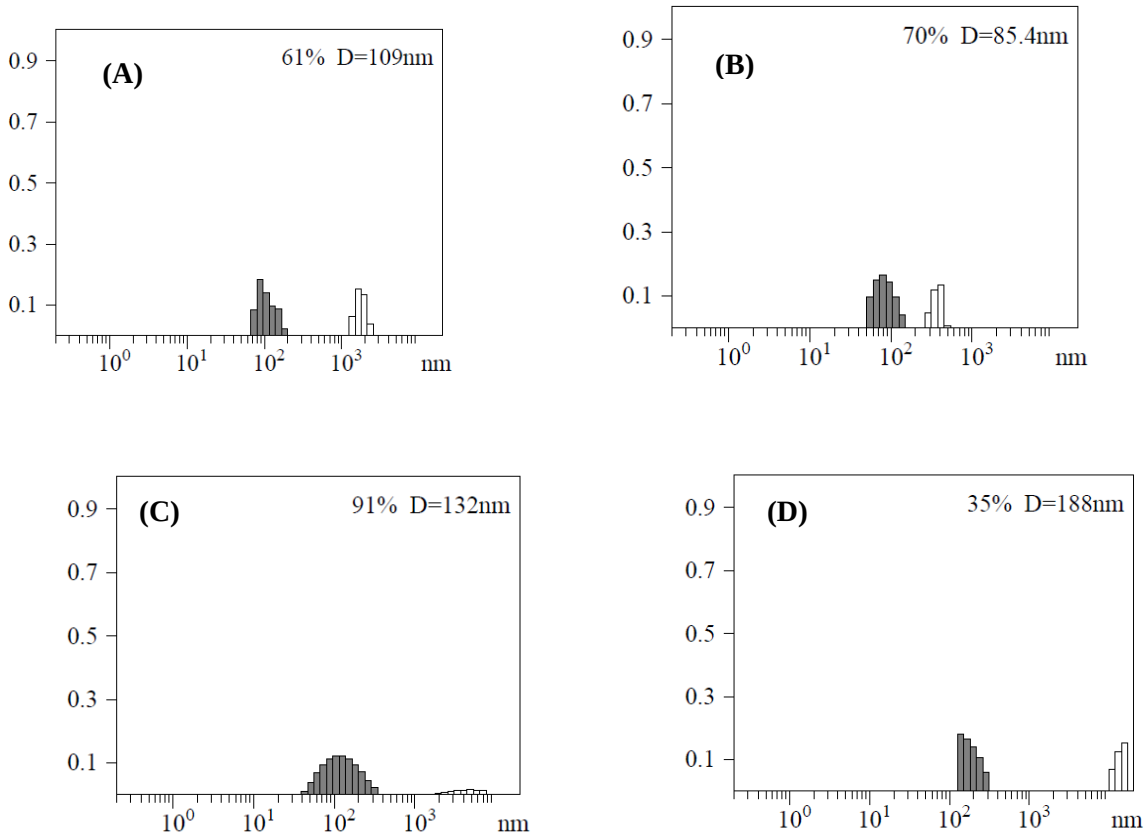

Figure 5. DLS of cross-linked liquid crystal with 5 percent photoinitiator (A) before washing with methanol, (B) after washing with methanol; with 20 percent photoinitiator (C) before washing with methanol and (D) after washing with methanol.

TEM and AFM

According to the results in the photocross-linking, 20 mol % of photoinitiator was used to obtain stable cross-linked materials. The materials were soluble in chloroform and studied by TEM and AFM. From TEM characterization (Figure 6), the cross-linked material was circular in shape and had two different sizes. The larger ones were 150- 200 nm in diameter, and the smaller ones were around 50 nm in diameter. To further explore the cross-linked material, AFM was applied to examine the height of the cross-linked materials. However, from AFM results (Figure 7) it is hard to make a solid conclusion. The cross-linked material was highly viscous and stuck to the detecting tip of the AFM. The contaminated tip then dragged the material everywhere. Hence, it is difficult to observe individual discs on a sample plate, as there was significant aggregation of the cross-linked material.

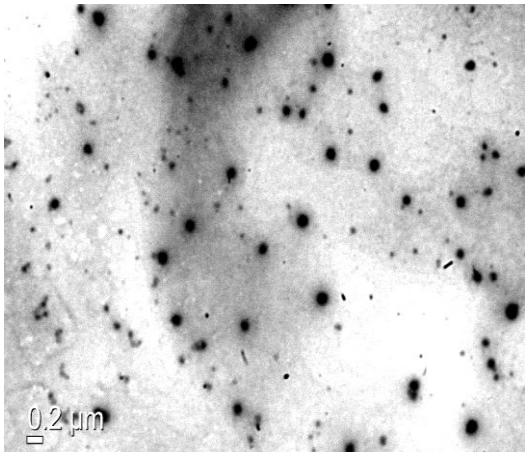

Figure 6. TEM of liquid crystal after being dissolved in organic solvent.

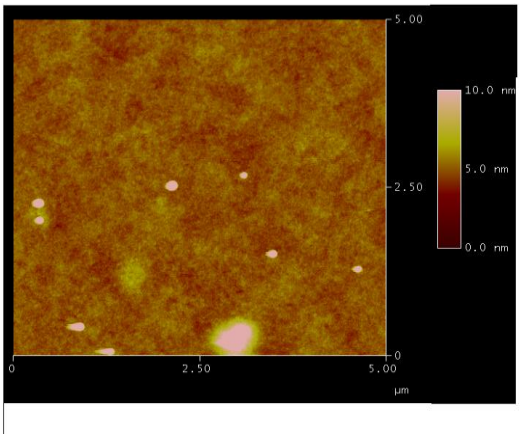

Figure 7. AFM of liquid crystal after being dissolved in organic solvent.

The cross-linked material was examined by TEM and AFM to distinguish the liquid crystalline structure of surfactant **5** between lamellar phase and SmA phase, too. Cross-linking in hydrophilic regions should give layer-like extended structures as well. On the other hand, the SmA phase consists of discs or cylinders, which arrange in layers. If surfactants are cross-linked via the hydrophilic headgroups in SmA phase, the cross-linked materials will be discs or cylinders with hydrophilic interiors. Taken all the data together, the liquid crystalline structure of surfactant **5** should be the SmA phase because the cross-linked material was circular in shape instead of layer-like structure in TEM characterization.

In conclusion, from XRD, PLM and TEM characterizations, compound **5** did not form the inverse hexagonal phase. Instead, it formed the SmA phase which is composed of discs with hydrophilic interiors that packed into layers (Figure 8).

The shape of a surfactant influences its packing parameter, which determines the type of liquid crystalline structure. According to Israelachvili,[3] a reverse micelle columnar structure forms when a surfactant's packing parameter is much larger than 1, because bulky

hydrophobic region of a cone-shaped surfactant would be exposed to solution in order to obtain closest packing. A lamellar structure forms when *Q* is 1, because cylindrical surfactants tend to pack into a layer for obtaining closest packing. When compound **5** and the Gin's surfactant (**1**) are compared, the difference in their shapes is obvious and can explain why surfactant **5** did not form H_{II}. Both surfactant **5** and the Gin's surfactant have very similar hydrophobic regions, but different hydrophilic headgroups. A carboxylate group was used in the Gin's surfactant, and the triallyl ammonium group in surfactant **5**. The size of the carboxylate group is small, helping maintain the size balance between the hydrophilic headgoup and the hydrophobic tails to obtain $Q > 1$ to form inverse hexagonal phase. A triallyl ammonium group is much larger than a carboxylate, so it is very possible to change the original packing parameter in the Gin's surfactant. In other words, the larger head group decreases the size difference between the hydrophilic headgroup and the hydrophobic tail and alters the shape of a surfactant from a cone to a cylinder. The packing parameter decreases as a result. The more cylindrical surfactant moves toward the lamellar packing structure instead from the inverted hexagonal packing. Because the three dodecyl tails of **5** are still much larger than the triallyl ammonium headgroup, meaning that the surfactant still prefers a reverse micellar structure. The reverse micellar disc structure was obtained as a compromise. A disc has two flat surfaces suitable for more cylindrical-like surfactants packing into a lamellar-likr structure. Furthermore, discs can pack into layered structures for closer packing between flat surfaces. That would explain why the d-spacing from XRD was 3.7 nm, a little bit larger than twice of the chain length of a twelve-carbon chain (1.67 nm) (Figure 8). The larger size of a headgroup can influence the packing also by lowering the charge density, which weakens the electrostatic interactions among the surfactants.

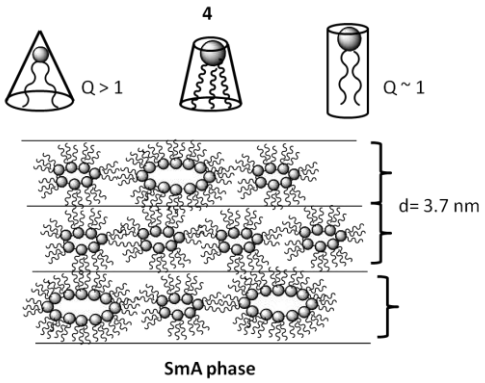

Figure 8. Demonstration of the shape of surfactant **4** compared with two surfactants with different Q values and demonstration how nanodiscs formed from **4** pack into layers.

Although triallyl(3,4,5-tridodecyloxybenzyl)ammonium bromide cannot successfully synthesize interfacially cross-linked organic nanotubes from a H_{II} liquid crystalline phase, further modification of the structure should afford desired results. It is known that the large trialllyl ammonium headgroup affects the packing parameter of surfactant. Hence, to increase the value of packing parameter without changing the headgroup, increasing the size of hydrophobic region is required. There may be several ways to increase the size of the hydrophobe, e.g. using branched hydrocarbon chains. Another way could be to add two extra carbons to each chain to increase the size of hydrophobic part a little bit, as done by the Kato group.[6]

2.5 Conclusions

Triallyl(3,4,5-tridodecylbenzyl)ammonium bromide was expected to form the inverse hexagonal phase because of its wedge like shape. Instead, it formed the smectic phase,

whose cross-linking afforded nanodiscs. The most likely reason for the phase change was the smaller packing parameter caused by the relatively large triallyl ammonium headgroup. The larger size of the triallyl ammonium group makes the shape more similar to cylindrical, but still maintains a cone shape. Therefore, the surfactants tend to undergo lamellar-like packing because they can pack more tightly, and the truncated cone-like surfactant helps them form the reverse micellar structure. The potential applications of the nanodiscs will be discussed in the next chapters.

2.6 Acknowledgements

The author would like to thank Dr. Brian Trewyn for allowing us to obtain the XRD characterization on his instrument and Dr. Robert Roggers for the assistance in the XRD characterization.

2.7 References

(1) Zhang, S.; Zhao, Y. *ACS Nano*. **2011**, *5*, 2637.

(2) (a) Dondoni, A. *Angew. Chem. Int. Ed.* **2008**, *47*, 8995. (b) Hoyle. C. E.; Lee, T.Y.; Roper, T. *J. Polym. Sci. Part A: Polym. Chem*. **2004**, *42*, 5301. (c) Iha, R.K.; Wooley, K.L.; Nystrom, A. M.; Burke, D.J.; Kade, M.J.; Hawker, C.J. *Chem. Rev*. **2009**, *109*, 5620.

(3) Israelachvili, J. N. *Intermolecular and Surface Forces with Applications to Colloidal and Biological Systems*. Academic Press. London, 1985. pp 229-274.

(4) Smith,R. C.; Fischer, W.M.; Gin, D.L. *J. Am. Chem.Soc.* **1997**, *119*, 4092.

(5) Kato, T.; Yasuda, T.; Kamikawa, Y.; Yoshio, M. *Chem. Commun*. **2009**, 729.

(6) Ichikawa, T.; Yoshio, M.; Hamasaki, A,; Taguchi, S.; Liu, F.; Zeng, X.-b.; Ungar, G.; Ohno, H.; Kato, T. *J. Am. Chem. Soc*. **2012**, *134*, 2634.

(7) Figueiredo Neto, A.M.; Salinas, S.A. *The Physics of Lyotropic Liquid Crystals: Phase Transitions and Structural Properties*. Oxford Science Press. New York. 2005.

(8) (a) Pindzola, B.A.; Jin, J.; Gin, D.L. *J. Am. Chem. Soc*. **2003**,*125*, 2940. (b) Mariani, P. *J. Mol. Biol*. **1988**, *204*, 165.

(9) Fujii, H.; Ohtaki, M.; Eguchi, K. *J. Am. Chem. Soc*. **1998**, *120*, 6832.

(10) Kohmoto, S.; Mori, E.; Kishikawa, K. *J. Am. Chem. Soc*. **2007**, *129*, 13364.

(11) Binnemans, K. *Chem. Rev*. **2005**, *105*, 4148.

(12) Duerr-Auster, N.; Kohlbrecher, J.; Zuercher, T.; Gunde, R.; Fischer, P.; Windhabs, E. *Langmuir*, **2007**, *23*, 12827.

(13) Kijima, T.; Ikeda, T.; Yada, M.; Machida, M. *Langmuir*, **2002**, *18*, 6453.

Chapter 3. TRANSPORT PROPERTIES OF NANODISCS FORMED FROM PHOTOCROSS-LINKING OF TRIALLYL(3,4,5-TRIDODECYLOXYBENZYL)AMMONIUM BROMIDE

3.1 Introduction

Facilitated transport of ions across bulk liquid membrane[1] has been widely applied and studied in separation[2] and purification of bioproducts.[3] Both cations and anions can be facilitated to transfer across an organic solution membrane (M) from one aqueous solution (feeding phase) to the other (stripping phase) by complexation in the organic phase. Carriers that are soluble in the organic phase can be chosen, designed, or modified to selectively form complexes with ions at one water-organic interface[4], which diffuse to the other water-organic interface, and release the ions into the stripping phase. The applications of carriers-mediated transport include in waste water treatment,[5] recovery and purification of pharmaceutical compounds,[6] separation of enantiomers,[7] and integrated process of reaction-separation in catalysis.[8]

The structures of the nanodiscs/ICRMs[9] make them potential carriers in phase transport. Both the nanodiscs and the ICRMs are covered with alkyl tails on their exteriors, making them soluble in organic solvents. The hydrophilic cores of both materials potentially can bind hydrophilic species. Charge selectivity is expected in the transport, as anions can easily complex with the cationic cores. Although the nanodiscs and the ICRMs possess similar structures, the nanodiscs are much larger structures and potentially might display different properties in the transport.

3.2 Experimental section

U-tube experiment[10]

A chloroform solution (15 mL) of the nanodiscs formed by surfactant **4** was added to a U-tube container. The concentration of the cross-linked surfactant was 0.1 mM. The appropriate aqueous solution of the dye (1.0 mM, 5 mL) and distilled water (5 mL) were added to the *cis*- and *trans*- side of the U-tube. Stirring speed was kept at 550 rpm. The *trans* phase was monitored by UV-VIS spectroscopy.

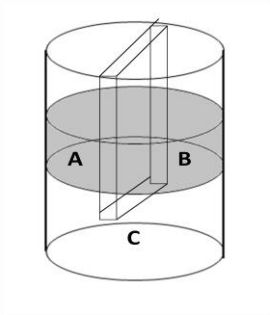

Figure 1. Set up for the U- tube experiment. A is the *cis* phase, B is the *trans* phase, and C is the liquid membrane.

3.3 Results and discussion

The U-tube experiment was set up as described in the literature (Figure 1).[3] The beaker used in the U-tube experiment had two partitions connected at the bottom. The carrier was dissolved in chloroform and placed at the bottom, and the two different aqueous solutions were then added on each side of the partition, respectively. One of the aqueous

solutions contained a water-soluble dye (the *cis* phase), and the other one distilled water (*trans* phase). The molar ratio of the water-soluble dye to the cross-linked surfactant in the nanodiscs or ICRMs was kept 10:1. Stirring was used to help the diffusion of the dye from the *cis* phase through the organic solution to the *trans* phase. The *trans* phase solution was monitored by UV-VIS spectroscopy as a function of time to determine the percentage of dye transferred from the *cis* phase.

3.3.1 Comparison of nanodisc and ICRMs

Alizarin red (**4**) was the first dye studied in the transport experiments. The first comparison was the transport efficiency among the triple-tailed nanodiscs (**1**), the double-tailed ICRMs (**2**), and the single-tailed ICRMs (**3**). The *trans* phase solution was monitored by UV-VIS spectroscopy as a function of time for 8 h, and the amount of dye transferred was calculated as percent transfer relative to the original amount of dye in the *cis* phase.

The transport results revealed that the triple-tailed nanodiscs (**1**) possessed higher efficiency than that of **2** and **3** in transporting anionic alizarin red across the liquid membrane. During transport, the organic solution turned red much faster with **1** in it than **2** or **3**. These results indicate that the nanodisc was quite permeable to the dye molecules.

One possible reason for the higher permeability of the nanodiscs could be a lower cross-linking density of the surfactants, making the core of the nanodiscs porous to molecule. A lower cross-linking density would also make the structure more flexible, allowing it to reconfigure itself at the water-organic interface to bind the hydrophilic guests. The same flexibility should also help the release when the complex diffuses to the *trans* phase.

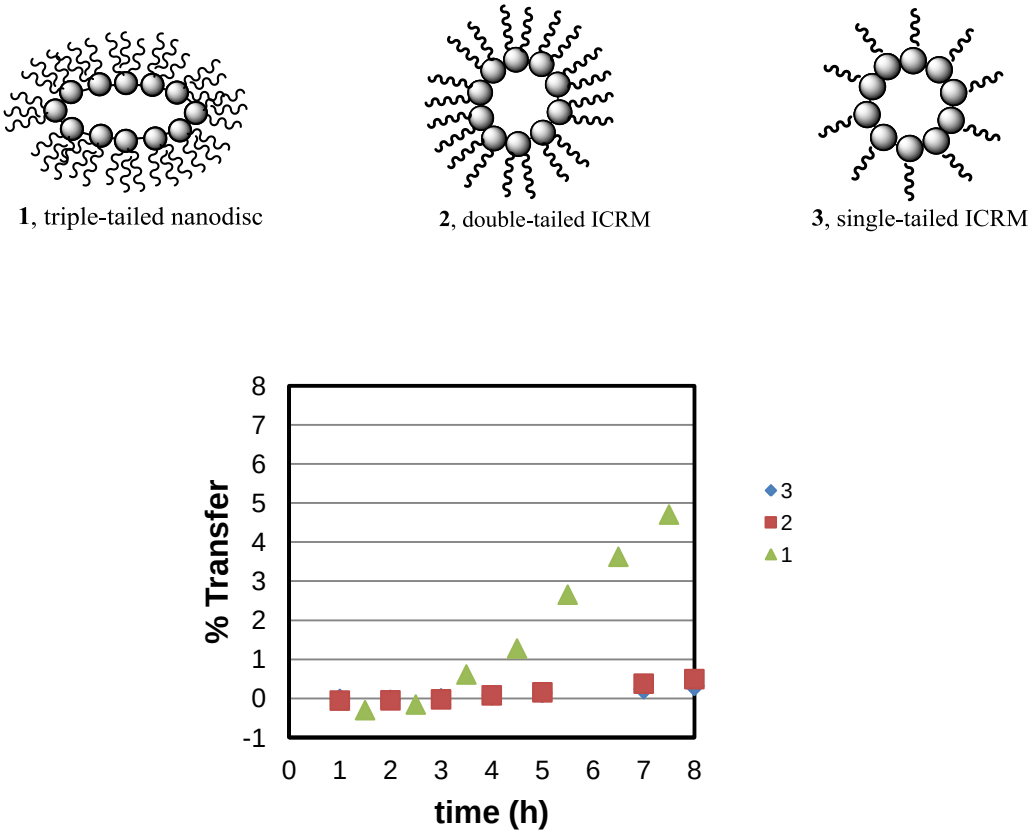

Figure 2. Comparison of single tailed ICRM, double tailed ICRM, and triple tailed discs.

3.3.2 Selectivity in Transport

The above results suggest that the nanodiscs formed from the triple-tailed surfactant were quite permeable to molecules of moderate size, possibly due to the low density on the cross-linking. It is likely that the core may be more permeable to some molecules than other due to either the difference in size or charge density.

With this possibility in mind, we investigated the transport of arsenazo III (**5**), a dye larger than alizarin red (**4**) and possessing more anionic groups. We also studied the transport of sodium 4-amino-1-naphthalenesulfonate (**6**), a molecule smaller than **4**.

As expected, the larger and more strongly anionic guest (**5**) showed nearly no transport at all. Not only so, the color of the organic phase displayed nearly no change after 24 h, suggesting that very little dye entered into the nanodiscs. It could be likely that the both large size of **5** and many anionic groups of **5** made it difficult to enter the core of the nanodiscs. Also, even for the dye that entered the organic phase, it never seemed to be released into the *trans* phase. The four strongly acidic groups of **5** (pK_1 = -2.5, pK_2 =0, pK_3 = pK_4 = 2.5)[11] suggest that the molecule is the multi-anionic form under our experimental conditions. The strong Columbic attraction between the anionic **5** and the cationic core may anchor the dye in the core of the nanodiscs, preventing its release.

As shown by Figure 3, guest **6** was transported faster than **4**. Thus, at the same charge density, the smaller guest was transported at a higher rate.

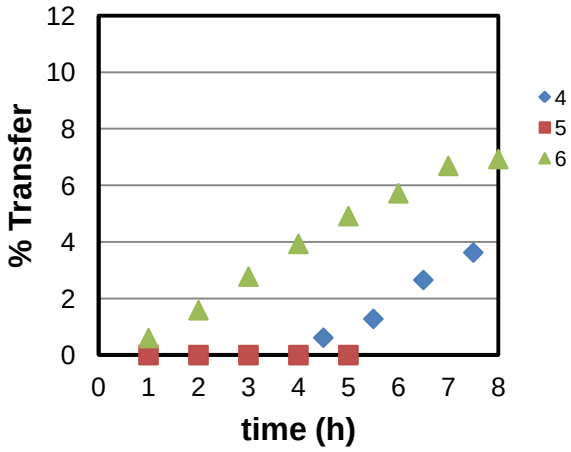

Figure 3. Size selectivity experiment in transport.

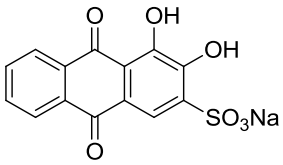

4 Alizarin red

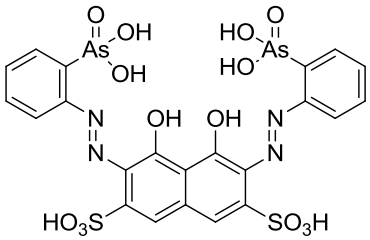

5 Arsenazo III

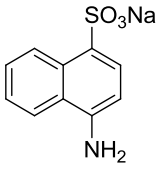

6 Sodium 4-amino-1-naphthalenesulfonate

3.3.3 Charge selectivity

The hydrophilic core of the nanodiscs consists of multiple cationic ammonium groups. The presumably low cross-linking density made the nanodiscs good transporters for molecules of moderate size (e.g. Alizarin red). Since the core is cationic in nature, we expect only anions can be transported. If a molecule's charge can be controlled, we should able to control the transport through the tuning of the electrostatic interactions between the molecule and the transporter.

Tryptophan is an amino acid, having both a carboxylic acid group (pKa= 2.38) and an amino group (pKa = 9.39). Its charge, therefore, can be controlled by the pH of solution. Under acidic conditions, tryptophan will carry a positive charge because both the carboxylate and amino group are protonated. In a basic aqueous solution, tryptophan will carry a negative charge because of carboxylate group. Tryptophan will be zwitterionic at neutral pH, making the molecule overall neutral.

The above hypothesis was confirmed in our transport experiments (Figure 4). When the transport was performed at pH = 3, 7, and 9, respectively, tryptophan was only transported at pH = 9. Clearly, neither neutral not cationic species can be transferred.

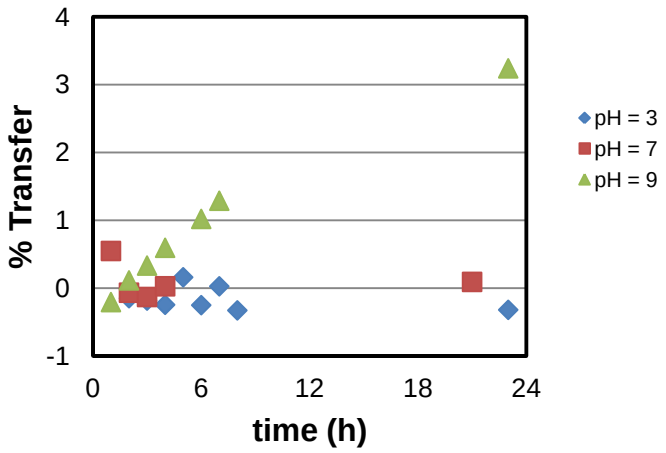

Figure 4. Charge selectivity of molecules in transport experiment.

3.4 Conclusions

The U-tube experiments showed that the nanodiscs are more efficient transporters than the ICRMs prepared from the single- and double-tailed surfactants. The study revealed the permeability of the core to molecules of moderate size (e.g. Alizarin red), possibly due to the relatively low cross-linking during the photocross-linking. When the guest gets too large and contains multiple anionic groups (i.e. Arsenazo III), the transport was shut down. Neither cationic nor neutral guests can be transported efficiently, consistent with the cationic nature of the core.

3.5 References

(1) (a) Maruyama, K.; Tsukube, H.; Araki, T. *J. Am. Chem. Soc.* **1982**, *104*, 5197-5203. (b) Behr, J.-P.; Kirch, M.; Lehn, J.-M. *J. Am. Chem. Soc.* **1985**, *107*, 241-246. (c) Yoshida, S.; Hayano, S. *J. Am. Chem. Soc.* **1986**, *168*, 3903-3907.

(2) (a) Calzado, J. A.; Palet, C.; Valiente, M. *Analytica Chemica Acta.* **2001**, *431*, 59-67. (b) Ensafi, A. A.; Eskandari, H. *Microchemical Journal* **2001**, *69*, 45-50.

(3) H. Reisinger, R. Marr. *J. Membr. Sci*. **1993**, *80*, 85-97.

(4) (a) Behr, J.-P.; Kirch, M.; Lehn, J.-M. *J. Am. Chem. Soc.* **1985**, *107*, 241-246. (b) Stolwijik, T.B.; Sudholter, E. J. R.; Reinhoudt, D. N. *J. Am. Chem. Soc.* **1987**, *109*, 7042-7047.

(5) (a) Yaftian, M. R.; Zamani, A. A.; Rostamnia, S. *Separation and Purification Technology.* **2006**, *49*, 71-75. (b) Kocherginsky, N. M.; Yang, Q. *Separation and Purification Technology*. **2007**, *54*, 104-116.

(6) Ishizu, H.; Habaki, H.; Kawasaki, J. *Journal of Membrane Science*. **2003**, *213*, 209-219.

(7) Breccia, P.; Gool, M. V.; P.-Fernandez, R.; M.-Santamaria, S.; Grago, F.; Prados, P.; de Mendoza, J. *J. Am. Chem. Soc.* **2003**, *125*, 8270-8284.

(8) (a) T.-Holownia, A.; Noworyta, A. *Journal of Membrane Science*. **2005**, *259*, 85-90. (b) Yang, F.; Wang, Y.; Guo, H.; Xie, J.; Liu, Zhiqiang. *Can. J. Chem.* **2010**, *88*, 622-627.

(9) (a) Zhang, S.; Zhao, Y. *ACS Nano*. **2011**, *5*, 2637. (b) Lee, L.-C.; Zhao, Y. *Organic Letters*. **2012**, *14*, 784.

(10) Sakai, N.; Matile, S. *J. Am. Chem. Soc*. **2003**, *125*, 14348.

(11) Rowatt, E.; Williams, R. J. P. *Biochem. J.* **1989**, *259*, 295-298.

Chapter 4: EXPLORATION OF APPLICATIONS OF NANODISCS IN CATALYSIS

4.1 Introduction

Enzymes are nature's prominent catalysts. They can carry out thousands of competing and often incompatible reactions selectively. The linear peptide chain can fold into the active structures with the catalytic site inside the enzyme, providing an isolated environment with different polarity from the aqueous solutions. These catalytic sites can select substrates by polarity, shape, size, and special functional groups to undergo specific reactions.

Materials to mimic enzymes' selectivity in reactions have attracted many researchers' attention. Materials spherical in shape and with a core-shell microstructure are amenable to mimicking enzymes,[1] as the shell can help isolate the catalytic site from the bulk solution.[2] Star polymers, for example, showed excellent site-isolation by their branched chains, providing internal microenvironments to incorporate incompatible catalysts used in tandem catalysis.[3]

Recently, the interfacially cross-linked reverse micelles (ICRMs) developed by the Zhao group was used as enzyme-like nanoreactor.[4] ICRMs were used as phase-transfer catalysts, having the phase-transfered anions located inside the hydrophilic nano-sized core, while the alkyl chains on the exterior can isolate the hydrophilic microenvironment from the organic solvent. The size selectivity of ICRMs can be controlled by the branching density (single-tailed or double-tailed surfactant) and the size of water pool. The structure of the cross-linked nanodiscs resembles that of the ICRMs. The nanodiscs should also be able to retain anions inside the core; the alkyl chains on the exterior can isolate the hydrophilic

interior from the organic solvent. In chapter 3, the U- tube experiments showed that the nanodiscs have charge (and possibly size) selectivity in the transport. Because the nanodiscs are larger and more permeable than the ICRMs, relatively large anions can enter and anchor inside the cationic core. In this chapter, organometallic catalysts with anionic ligands were incorporated into the core of nanodisc. The experiment was that, not only the nanodisc would act as a soluble support for the catalysts with potential selectivity, but also the strong electrostatic interactions between the nanodisc and the catalysts would prevent catalyst's decomposition through the dimerization process.[5,6]

4.2 Experimental section

Synthesis of Mn-TPPS complex[7]

5,10,15,20-Tetraphenyl-21*H*, 23 *H*-prophine-*p,p',p'', p'''*-tetrasulfonic acid tetrasodium hydrate (TPPS, 46.2 mg, 0.045 mmol) and $MnCl_2 \bullet 4\ H_2O$ (101.3 mg, 0.51 mmol) were dissolved in 1.2 mL of DMF. The reaction mixture was heated to reflux at 155 ^oC for 2 h, until UV absorption of the free TPPS disappeared (red shift from 415 nm to 467 nm, Figure 1). The mixture was cooled down to room temperature and the DMF was removed under vacuum. Mn-TPPS was precipitated in 5 mL of acetone. The black precipitate was collected by centrifugation. To remove the excess $MnCl_2$, the solid was dissolved in methanol and precipitated in acetone four times (26 mg, 61 %).

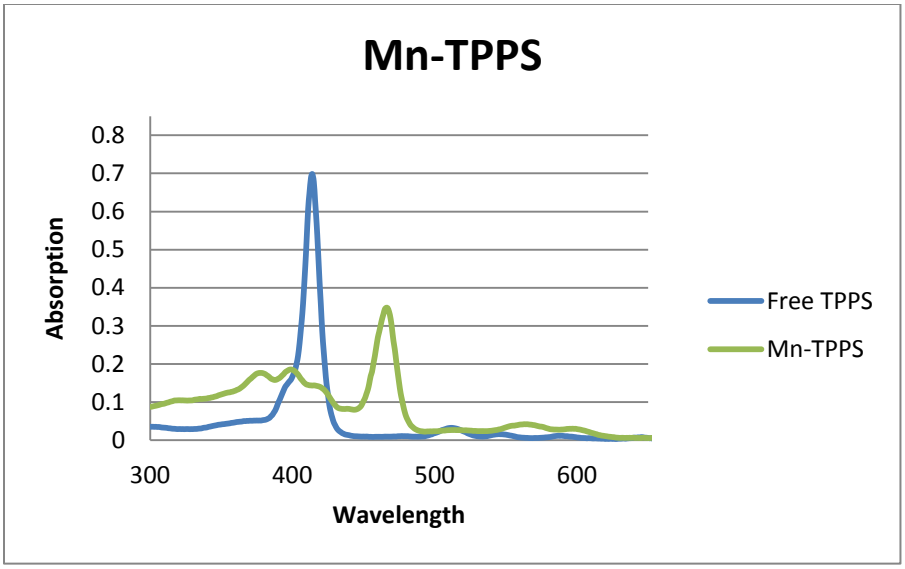

Figure 1. UV-vis absorption of free TPPS and Mn-TPPS complex.

General procedure of incorporation of water soluble catalyst into interfacially cross-linked discs

The water-soluble catalyst was dissolved in distilled water and discs were dissolved in chloroform and both solutions were added to a 1 dram vial containing a stir bar. The aqueous layer and organic layer were vigorously stirred for overnight and incorporation is complete as the aqueous layer changed to colorless.

Mn porphyrin complex catalyzed epoxidation

The stock solution of the Mn-containing nanomaterial and the alkene substrates in chloroform were prepared. A hydrogen peroxide aqueous solution was added to the chloroform solution in a 1 dram vial. The mixture was stirred vigorously at room temperature for 12 h. The conversion of the reaction was determined by ^{1}H NMR spectroscopy.

4.3 Results and discussion

Mn-catalyzed epoxidation

An anionic porphyrin with four sulfonate groups was selected as the ligand to coordinate with Mn. The Mn-porphyrin complex permeates into the nanodiscs and is fixed inside the cationic core via Columbic interactions between the sulfonate groups and the ammonium headgroups of the nanodiscs. The catalyst loading was varied, with the idea that a low loading would make it more difficult for two metalloporphyrin to dimerize. Table 1 shows the catalytic results with [Mn]/[surfactant] ratio at 1/80.

Table 1. Epoxidation catalyzed by Mn-TPPS in the interfacially cross-linked discs.

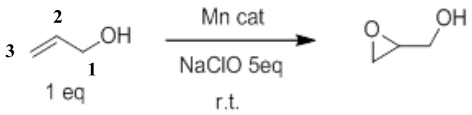

entry[a]	cat (mol%)	[Mn]/[surfactant]	anion	t (h)	% conversion
1	1	1/80	Br-	12	**86**
2	0.1	1/80	Br-	12	**95**
3[b]	0	0	Br-	12	**81**

[a]The reaction was a biphasic reactions; with NaClO in aqueous phase and the catalyst and substrate in d-chloroform layer. The percent conversion was determined by ^{1}H NMR spectroscopy. [b]Entry 3 is blank test, the mol % of surfactant 5 is 0.08.

The Mn-porphyrin catalyst at 1 mol % level with 1:80 ratio of Mn to surfactant gave high conversion of allyl alcohol (entry 1). To explore the catalytic efficiency of the Mn-porphyrin catalyst in epoxidation, the amount of Mn was decreased to 0.1 mol % with respect to allyl alcohol and the ratio of Mn to surfactant was maintained at 1:80. To our surprise, high percent conversion of allyl alcohol was still obtained (entry 2). The effect of the anion was also explored as the size and charge of the anions may also influence site-isolation of the catalysts.

To our surprise, 81 % conversion was obtained without Mn-porphyrin catalyst (entry 4). Because there is no epoxidation catalyst added in the nanodisc, it could be possible that the ammonium headgroups were responsible for the catalysis. In the literature, some epoxidation reactions can be carried out by quaternary ammonium salts. For example, enantioselective epoxidation of α,β-enone can be catalyzed be asymmetric quaternary ammonium salt.[8] The proposed charge-accelerated mechanism is that the anionic oxygen of α,β-enone conjugate (enolate oxygen) is stabilized by cationic ammonium through the Columbic attraction, and the oxidant (OCl^-) was attracted to the α,β-enone substrate through ion-paring.

The epoxidation catalysis in the nanodiscs possibly follows a similar mechanism. The nanodisc is composed of ammonium headgroups. These ammonium groups could concentrate the anionic hypochlorite to the core, enhancing its reactivity. The hydrophilic core might also have concentrated the hydrophilic allyl alcohol. Possibly, both the higher effective concentrations of the reactants in the core and the electrostatic interactions between

the ammonium group and the hypochlorite were responsible for the catalysis. More experiments are needed to reveal the epoxidation mechanism catalyzed by the nanodiscs.

4.4 Conclusions

Mn-porphyrin catalyst can be site-isolated inside the large core of the nanodisc by Columbic interactions. However, the epoxidation of allyl alcohol can also be carried out without Mn-porphyrin catalyst but with the ammonium headgroups of the nanodisc.

4.5 Acknowledgement

The author would like to thank Dr. Isaac Ho for discussing Rh catalyzed hydrogenation mechanism and property of Rh catalyst.

4.6 References

(1) (a) Tomalia, D. A.; Frechet, J. M. J. *Prog. Polym. Sci.* **2005**, *30*, 217-219. (b) Voit, B. *J. Polym. Sci., Part A: Polym. Chem.* **2000**, *38*, 2505-2525.

(2) (a) Harth, E.M.; Hecht, S.; Helms, B.; Malmstrom, E. E.; Frechet, J. M. J.; Hawker, C.J. *J. Am. Chem. Soc.* **2002**, *124*, 3926-3938. (b) Zhao, M.; Helms, B.; Slonkina, E.; Friedle, S.; Lee, D.; DuBois, J.; Hedman, B.; Hodgson, K.O.; Frechet, J. M. J.; Lippard, S. J. *J. Am. Chem. Soc.* **2008**, *130*, 4352-4363.

(3) (a) Dichtel, W. R.; Baek, K.-Y.; Frechet, J. M. J.; Rietveld, I. B.; Vinogradov, S. A. *J. Polym. Sci. Part A: Polym. Chem.* **2006**, *44*, 4939-4951. (b) Bosman, A. W.; Heumann, A.; Klaerner, G.; Benoit, D.; Frechet, J. M. J.; Hawker, C.J. *J. Am. Chem. Soc.* **2001**, *123*, 6461-6462.

(4) Lee, L.-C.; Zhao, Y. *Organic Letters*. **2012**, *14*, 784.

(5) (a) Kochi, J.K.; Michaud, P.; Srinvasan, K. *J. Am.Chem. Soc*. **1986**, *108*, 2309. (b) Shultz, A.M.; Sarjeant, A. A.; Farha, O. K.; Hupp, J. T.; Nguyen, S.T. *J. Am. Chem. Soc*. **2011**, *133*, 13252.

(6) (a) Merlau, M. L.; Grande, W. J.; Nguyen, S. T.; Hupp, J. T. *Journal of Molecular Catalysis A: Chemical*. **2000**, *156*, 79. (b) Morris, G. A.; Ngyuen, S. T.; Hupp, J. T. *Journal of Molecular Catalysis A: Chemical*. **2001**, *174*, 15. (c) Merlau, M.L.; del Pilar Mejia, M.; Ngyuen, S.T.; Hupp, J. T. *Angew. Chem. Int. Ed*. **2001**, *40*, 4239.

(7) Granados- Oliveros, G.; Paez-Moza, E.A.; Ortega, f.M.; Piccinato, M.T.; Silva, F. N.; Guedes, G. L. B.; Di Mauro, E.; da Costa, M. F.; Ota, A.T. *Journal of Molecular Catalysis A: Chemical*. **2011**, *339*, 79.

(8) Corey, E.J.; Xu, F.; Noe, M. C. *J. Am. Chem. Soc*. **1997**,*119*, 12414.

Chapter 5: CONCLUSIONS

Triallyl(3,4,5-tridodecyloxybenzyl)ammonium bromide was expected to form H_{II} phase because of its wedge-like shape. Instead, it formed smectic phase, which afforded interfacially cross-linked nanodiscs after photocross-linking. The most possible reason was the large size of triallyl ammonium headgroup that which decreased the packing parameter, making the surfactant more cylindrical. The amphiphiles then preferred the lamellar-like packing, while the surfactant maintaining the truncated cone-shape, affording the reverse micellar structure.

The nanodiscs can be used as transporters in facilitated transport of ions across bulk liquid membrane. The nanodiscs were quite efficient at transporting molecules of moderate size (e.g. Alizarin red), possibly due to the relatively low cross-linking density among surfactants. Anions were transported more efficiently than neutral and cationic guests because of the electrostatic attraction between the anions and the cationic core of the nanodiscs. The cross-linked material was also used as catalyst support for anionic Mn-porphyrin; however, the epoxidation of allyl alcohol was found to be observed even by the nanodiscs, possibly because of ammonium headgroups and hypochlorite only.

APPENDIX

Compound **5**

^{1}H-NMR ($CDCl_3$)

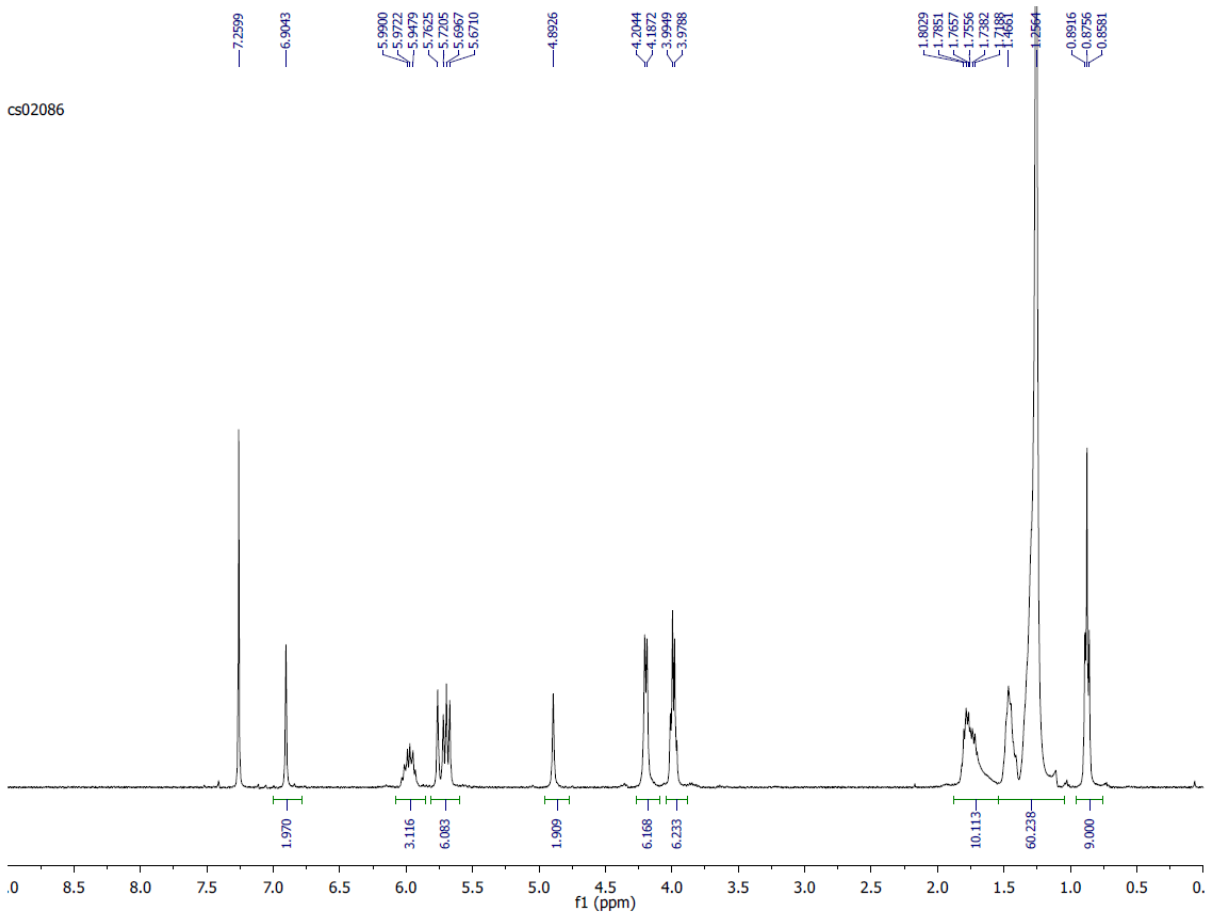

Compound **5**

^{13}C-NMR ($CDCl_3$)

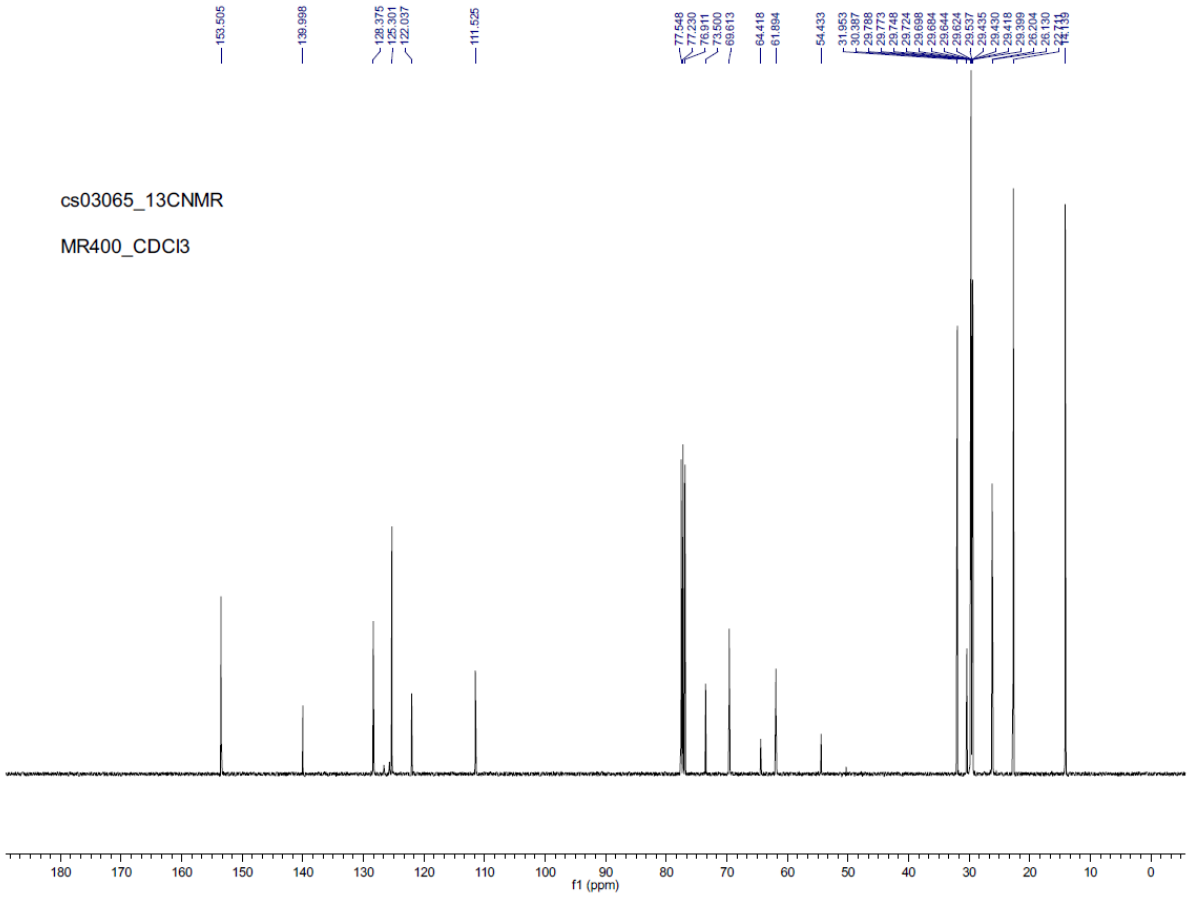

Compound **6**

^{1}H-NMR ($CDCl_3$); Identified impurities: dimethylformamide (DMF)

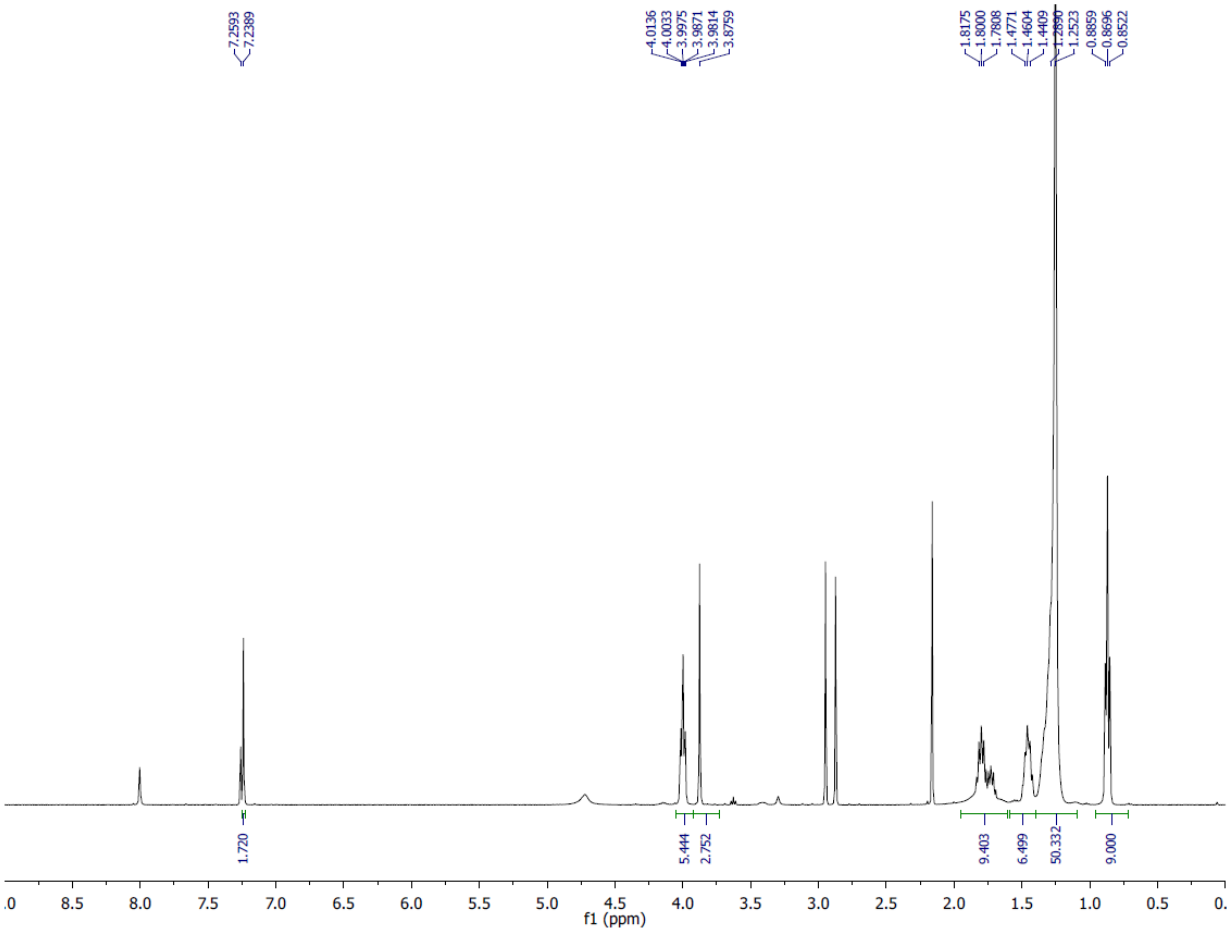

Compound **7**

^{1}H-NMR ($CDCl_3$); Identified impurities: tetrahydrofuran.

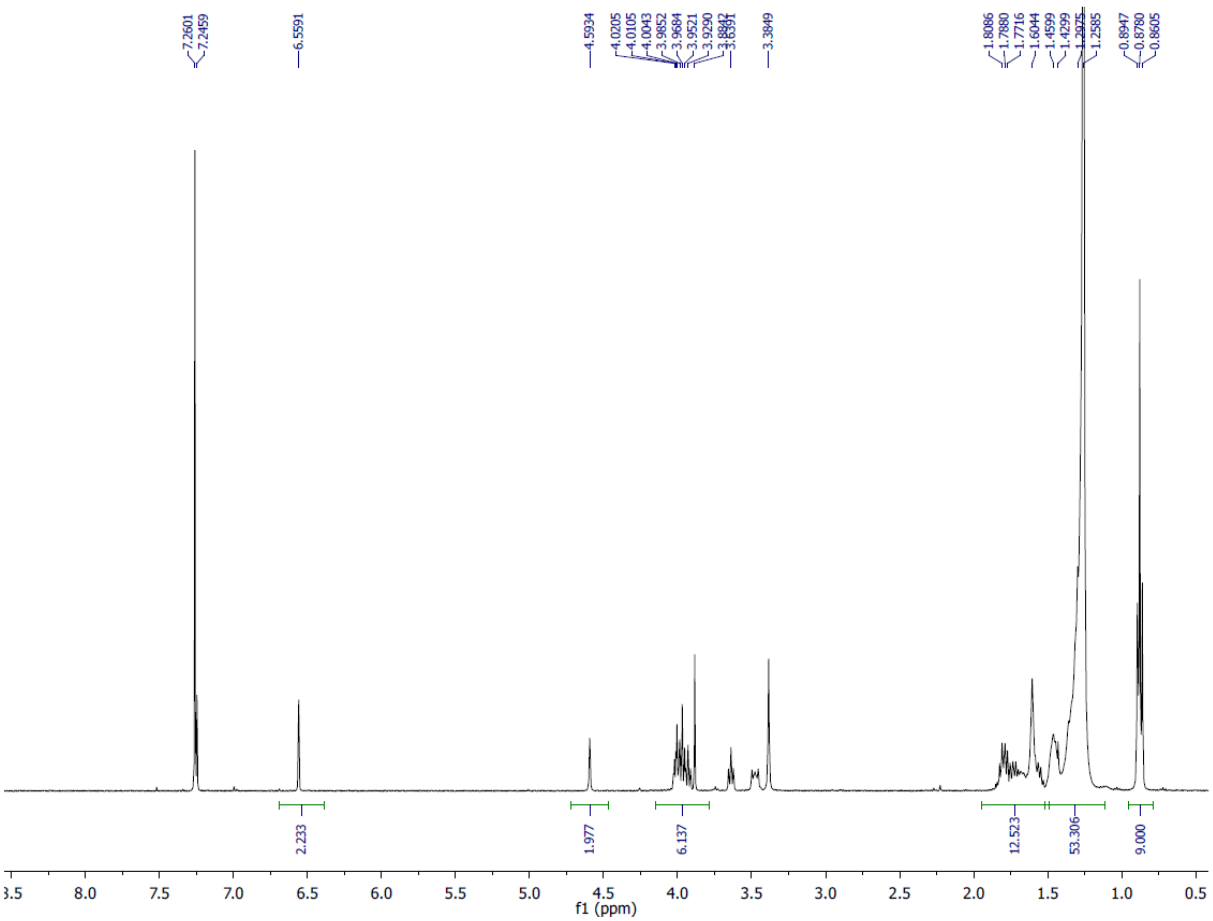

Compound **8**

^{1}H-NMR ($CDCl_3$)